Veterinary Parasitology 193 (2013) 413–426

Contents lists available at SciVerse ScienceDirect

Veterinary Parasitology

journal homepage: www.elsevier.com/locate/vetpar

Lung histopathology, radiography, high-resolution computed tomography, and bronchio-alveolar lavage cytology are altered by *Toxocara cati* infection in cats and is independent of development of adult intestinal parasites

A. Ray Dillon*, D.M. Tillson, J. Hathcock, B. Brawner, A. Wooldridge, R. Cattley, B. Welles, S. Barney, T. Lee-Fowler, L. Botzman, M. Sermersheim, R. Garbarino

Auburn University, College of Veterinary Medicine, Auburn, AL, United States

ARTICLE INFO

Keywords:
Toxocara cati
Pulmonary fibrosis
High resolution CT
Larval migration

ABSTRACT

This study presents clinical findings after oral ingestion of *Toxocara cati* eggs which resulted in rapid pulmonary lung migration and parenchymal disease, noted on clinically relevant diagnostic methods. Further, the study investigated the efficacy of pre-infection applications of preventative medication on larval migration through the lungs. A third aim of the study was to determine if adult cats infected with *T. cati* developed lung disease. Cats in infected groups were administered five oral doses of L3 *T. cati* larvae. Four-month-old specific pathogen free (SPF) kittens were divided into three groups (six per group): an infected untreated group, an uninfected untreated control group, and an infected treated group (topical moxidectin and imidacloprid, Advantage Multi for Cats, Bayer Healthcare LLC). Six 2- to 3-year-old adult multiparous female SPF cats were an infected untreated adult group. The cats were evaluated by serial CBCs, bronchial–alveolar lavage (BAL), fecal examinations, thoracic radiographs, and thoracic computed tomography (CT) scans and were euthanized 65 days after the initial infection.

Adult *T. cati* were recovered in infected untreated kittens (5/6) and infected untreated adults (5/6) in numbers consistent with natural infections. Eggs were identified in the feces of most but not all cats with adult worm infections. No adult worms were identified in the uninfected controls or the infected treated group. All cats in the infected groups, including treated cats and untreated cats without adult worms, had lung pathology based on evaluation of radiography, CT scans, and histopathology.

The infected cats demonstrated a transient peripheral eosinophilia and marked eosinophilic BAL cytology, but normal bronchial reactivity based on in vivo CT and in vitro ring studies. Lung lesions initially identified by CT on day 11 were progressive. Thoracic radiographs in infected cats had a diffuse bronchial–interstitial pattern and enlarged pulmonary arteries. Pulmonary arterial, bronchial, and interstitial disease were prominent histological findings. Infected treated cats had a subtle attenuation but not prevention of lung disease compared to infected cats. Significant lung disease in kittens and adult cats is associated with the early arrival of *T. cati* larvae in the lungs and is independent of the development of adult worms in the intestine. These data suggest that while the medical prevention of the development of adult parasites after oral exposure to *T. cati* is obviously beneficial, this practice even with good client compliance will not prevent the development of lung disease which can alter clinical diagnostic methods.

* Corresponding author at: College of Veterinary Medicine, Auburn University, Auburn, AL 36849, United States. Tel.: +1 334 844 4690.
E-mail address: dilloar@auburn.edu (A.R. Dillon).

0304-4017
http://dx.doi.org/10.1016/j.vetpar.2012.12.045

1. Introduction

Respiratory clinical signs are a common reason for cat owners to present their cat for veterinary care and the diagnostic evaluation may include thoracic radiographs, peripheral blood CBC, and a bronchial–alveolar lavage for cytology.

The veterinary profession has advocated preventive medications for intestinal parasitism with the adult parasite as the target (Bowman, 2009; Epe, 2009; Companion Animal Parasite Council, 2012; European Scientific Counsel Companion Animal Parasites, 2006; Little, 2011). Regardless of the region of the United States, approximately 25% of all shelter cats have positive fecal examinations for eggs of *Toxocara cati* (Nutter et al., 2004; Blagburn, 2010) and this infection is common in client owned cats (Nolan and Smith, 1995; Blagburn et al., 1996; Spain et al., 2001; DeSantis et al., 2006; Little et al., 2009). Although incidence in other areas of the world can vary (Martínez-Barbabosa et al., 2003; Gates and Nolan, 2009; Mircean et al., 2010; Borthakar and Mukharjee, 2011), it may be assumed that infective eggs are available to most cats (Sommerfelt et al., 2006; Macuhova et al., 2010; Fahrion et al., 2011). The role of *T. cati* infections in inducing lung disease has not been carefully defined as related to timing or nature of the lung pathology and effects on diagnostic modalities, such as complete blood count (CBC), radiographs, computed tomography (CT) analysis, and bronchial alveolar lavage (BAL) cytology. Experimental evidence that *T. cati* can induce significant pulmonary arterial disease and interstitial lung disease (Sprent, 1956; Swerczek et al., 1970) suggest that *T. cati* larval migration is a potential cause of lung pathology, which may be clinically relevant to clinical presentation and diagnostic testing. The role of *T. cati* larval migration to initiate lung disease that may be progressive formed the basis of this investigation.

The detection of severe lung parenchymal disease in randomly sourced cats, where an ascarid had been detected in the lung sections, has renewed interest in the role of *T. cati* in feline lung disease (Upchurch et al., 2010). The lung is central to the systemic migration of *T. cati* larvae associated with oral ingestion of the eggs and lung migration is not generally understood to occur though oral ingestion of earthworms, cockroaches, or rodents, or by lactogenic transmission in the queen after acute infections during late gestation (Sprent, 1956; Coati et al., 2004; Bowman, 2009). The timing of the larval emergence from eggs and migration of the L3 larvae through the gastric wall to the visceral organs and liver, then to the pulmonary arterial beds, is not predictable in the cat, but is assumed to occur within a few days to weeks (Sprent, 1956). The duration of the lung phase is difficult to determine, as lung changes are residual with no presence of the larvae in lung histopathology. Furthermore, the timing and location of the *T. cati* L3 to L4 molt has not been determined in the cat. Repeated serial infections in cats resulted in progressively more severe lung pathology in kittens as compared to a single large dose and an exaggerated host response to subsequent infections has been suggested (Swerczek et al., 1970). Prevention of roundworm infections after oral exposure has been based on the absence of adult (L5) stages in the intestine, but the effects of preventive medications on larval stages has not been defined (McTier et al., 2000; Arther et al., 2005; Reinemeyer et al., 2005; Schenker et al., 2007; Wolken et al., 2009; Petry et al., 2011; Yildiz et al., 2011).

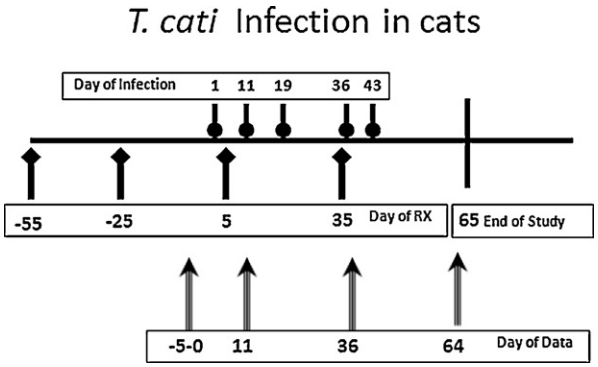

Fig. 1. *T. cati* Infection in cats study design. Oral infective L3 of *T. cati* were administered on days 1, 11, 19, 36, and 43 to infected untreated cats (6), infected treated cats (6), and infected untreated adult cats (6). Treatment with a preventive medication was initiated on day −55, −25 before the infection and on days 5 and 35 after the infection in treated cats (6). CBC, bronchio-alveolar lavage cytology, radiographs, and CT scans were performed before the infection day and days 11, 36, and 64 after the infection.

The hypothesis of this study was that oral ingestion of *T. cati* eggs would result in rapid pulmonary lung migration inducing lung parenchymal disease that will be noted using clinically relevant diagnostic methods. The study also determined if preinfection applications of topical moxidectin and imidacloprid (Advantage Multi for Cats, Bayer Animal Health LLC, Kansas City) would prevent larval lung migration. Thirdly, the study was designed to ascertain if adult cats infected with *T. cati* would develop lung disease associated with larval migration.

2. Materials and methods

2.1. Experimental design

Four-month-old specific pathogen free (SPF) kittens (mean BW 2.8 kg) were randomly divided into three groups of six per group: an infected untreated group (IU), an uninfected untreated control group (UU), and an infected treated group (IT) which received topical 4 mg moxidectin and 40 mg imidacloprid at the label dose (Advantage Multi for Cats, Bayer Animal Health LLC, Animal Division, Kansas City). Relative to the first infective dose of *T. cati*, IT cats were medicated on days −55, −25, 5, and 35 (Fig. 1). Cats in all infected kitten groups were administered five oral doses (2000 L3 *T. cati* larvae/dose) on days 1, 11, 19, 35, and 42, which were voluntarily consumed. An additional group of six adult (2- to 3-year-old) multiparous female SPF cats (2.8–4.1 kg) formed an infected untreated adult (IUA) group. Adult cats were infected and evaluated on the same time sequence as kittens, except the infective dose at each time was 1000 L3 *T. cati* larvae. Relative to the first infective dose of *T. cati* (day 1), cats were serially evaluated on day 0 for baseline (data collected from day −14 to day −5), and again on days 10 and 11, days 36 and 37, and

day 64 for the progressivity of the lung disease. Evaluation included peripheral CBC and differential, cytologic evaluation of bronchio-alveolar lavage (BAL) fluid recovered from 10 ml of lactated Ringer's solution, thoracic radiographs, and thoracic CTs. Fecal samples were examined weekly from day 45 to day 64 in cats for parasite eggs (Parasite Diagnostic Laboratories, Auburn University, AL). All statistical analysis of data was performed with Systat Software (SigmaPlot 12, Systat Software, Inc., 1735 Technology Drive, Suite 430, San Jose, CA 95110). The protocol was approved by the Auburn University Institutional Animal Care and Use Committee. Cats were acclimated and housed in study groups in an AAALAC accredited facility (AAALAC International, MD, USA). For the day of procedures the cats were sedated with an intramuscular dose of medetomidine (Dormitor, Pfizer Animal Health, NY), butorphanol (Torbugesic, Fort Dodge, IA), ketamine (ketamine hydrochloride, Abbott Lab, Chicago, IL) and after the procedures an intramuscular dose of atipamizole (Antisedan, Pfizer Animal Health, NY) was administered. Cats were monitored daily and physical examinations performed weekly.

2.2. CBC and BAL cytology

Peripheral blood for CBC was submitted for routine analysis. BAL fluid was concentrated and the cytology was evaluated and the cell type identified reported as a percentage of total cells observed (Clinical Pathology Diagnostic Services, College of Veterinary Medicine, Auburn University, AL).

2.3. Digital radiographs

Digital radiographs obtained at multiple points (days 0, 11, 35, 64) were graded for severity of lung lesions. Radiographs were scored for pulmonary artery, bronchial pattern, interstitial pattern, and mixed bronchio-interstitial–alveolar pattern using a 0–3 system (0 = none and 3 = severe lesions). In addition, any abnormalities in cardiac, pleura, or diaphragm were recorded. Scores were compared by paired *t*-tests for changes within groups over time and by ANOVA for differences between groups of cats.

2.4. CT acquired images

On days 0, 11, 36, and 64, pulmonary CT images were acquired with a helical CT scanner (helical CT scanner, General Electric Co., Milwaukee, WI). Examinations were performed with cats in sternal recumbency under general isoflurane (0.5–0.75%) inhalational anesthesia (Isoflurane, USP, Piramal Healthcare, Ltd., AP Andhra Pradesh, India) using a breath hold technique (airway pressure maintained at 14 cm of water) (Reid et al., 2012). Images of the entire lung field were obtained consisting of contiguous, 5-mm collimated transverse images, and thin-slice axial scans (1-mm collimated transverse images) spaced 10 mm apart. A non-iodinated intravenous contrast (Isovue-370 Iopamidol Injection 76%, Bracco Diagnostics Inc., Princeton, NJ) at a dose of 0.5 ml/lb was administered before contrast image acquisition. 1 mm transverse sequential CT images of the lung were acquired and reconstructed using a detail and bone algorithm. The CT scans were graded (0–3 scale) as adapted from human and canine studies (Johnson et al., 2004, 2005). For CT evaluation, images were viewed in a lung window (W 1500, L 600).

2.4.1. Lung density by Hounsfield units

The DICOMM images of the CT scans were imported onto the 3D Slicer software (www.Slicer.org, Version 2.8). Density mask analysis of the lung parenchyma was performed based on the contiguous 1-mm thin-section images. In the software, automatic extraction of the lung is achieved by performing thresh holding using the Otsu Method (Otsu, 1979). The CT slices were exported into the COPD-Emphysema module, and lung density histograms were obtained ranging in Hounsfield units (HU) of −300 to −1000. Distribution curves were generated for each and the frequency of HU at −600, −856, −910, −925, and −950 were calculated.

2.4.2. Lung width

At fixed inspiratory pressure of 14 cm H_2O, the CT image cross-sectional diameter was measured. At the level transverse to the caudal lung lobe just behind the cardiac apex, at the level before the third bronchiole separates off the right main bronchus, the diameter of the chest wall was measured. The measurement (efilm 2.1, Merge Healthcare, Milwaukee, WI) was a straight line at the base of the esophagus extending the width of the lungs. With day 0 measurement as its own control, the percentage change from day 0 to day 64 for each cat was calculated.

2.5. In vivo bronchial ring reactivity

Bronchial ring reactivity in vivo was evaluated using sequential 1 mm CT scans (described above) obtained at baseline, after methacholine (Provocholine, Methacholine Chloride USP) 100 mg powder (manufactured by Pancap for Methapharm, Inc., Brantford, Ontario, Canada), nebulization (30 mg/cat for 2 min via endotracheal tube), and again after albuterol (Albuterol sulfate inhalation solution, 0.083% 2.5 mg/3 ml, The Ritedose Corp for Sandoz, Inc., 1 Technology Circle, Columbia, SC) nebulization (25 mg/cat for 2 min via endotracheal tube). The bronchial diameters were measured on a 1-mm slice at the level of the right caudal lung bronchi, just caudal to the apex of the heart and before the third bifurcation. Baseline bronchial areas and diameter measurements for each cat were compared to the diameter after methacholine and after albuterol challenge and expressed as percentage change from baseline. The bronchial ring size was evaluated by both cross-sectional area using OxiriX (MacPro, Apple Inc.) and direct caliper measurement of interior diameter of the bronchi at the air/wall interface.

For evaluation of effects of albuterol nebulization on contracted airways, on day 64 the uninfected untreated cats (UU) were evaluated after breathing only oxygen for 5 min after the completion of the methacholine CT scans, and then the albuterol nebulization was performed and CT scans again performed.

2.6. Necropsy

Cats were euthanized (Euthasol, Virbac Animal Health, P.O. Box 162059 Fort Worth, TX) on day 65 after the initial infection with barbiturate; the intraperitoneal route of injection was utilized to avoid pulmonary artifacts induced by additives in the euthanasia solution. Tissue samples of intestine, liver, kidney and lung were obtained. The right caudal lobe was formalin fixed by infusion into the main bronchus to an inflation pressure of 12 cm H_2O and the bronchus was ligated to maintain expansion for processing. Adult worms in the intestine were collected for determination of sex and size.

2.7. In vitro bronchial ring reactivity

From the left caudal lung lobe, bronchial rings were collected for bronchial ring reactivity via in vitro challenge. Isometric force of epithelium-intact third- to fourth-generation intra-parenchymal bronchioles (IPBs) (internal diameter, 300 to 500 μm) from IU and UU cats was performed as described (Wooldridge et al., 2012).

2.8. Histopathology

Multiple sections of fixed-perfused right caudal lung were stained with H&E and α-smooth muscle actin (HSRL Inc., Mount Jackson, VA 22842). Sections were scored on a scale of 0–3 separately for interstitium, bronchioles, bronchus, pulmonary arterioles, and major pulmonary artery areas. The right caudal lung at the mid-lobar cross-section, corresponding to the CT slice used for in vivo bronchial ring reactivity, was evaluated. Also, a minimum of five pulmonary arterioles and five bronchioles were photographed and the area of the lumen, total area, and wall thickness were measured (open source software program, Image J, www.NIH.org). For each lung, the lumen/wall, wall thickness/lumen, and total area/lumen ratios were calculated.

2.9. Correlation of diagnostic findings

For statistical analysis (SigmaPlot 12, Systat Software, Inc.), when abnormalities were demonstrated, correlation coefficients were evaluated for variables (peripheral eosinophilia, eosinophil increases on BAL, positive fecal examinations, presence of adult *T. cati*, CT lesions and scores, radiographic scores and histopathology scores) both within study groups and between study groups.

3. Results

3.1. Consequences of diagnostic procedures and patency of infection

All cats were asymptomatic for any clinical disease during the observation period and there were no adverse effects of the serial diagnostic methods. At the time of necropsy, examination of the intestinal tract demonstrated adult worms in 0/6 of the UU cats, 5/6 of the IU cats, and O/6 of the IT cats. The cats with adult worms demonstrated different sizes of *T. cati* reflecting serial timing of the infections. In the IUA cats, 5/6 had *T. cati* in the intestine (Table 1). Examination of all weekly fecal samples revealed eggs in only 4/6 IU and 4/6 IUA group animals.

Table 1
Results of *T. cati* infections: adult recovery and fecal results.

Cat ID	Males	Females	Immature	Total frags	Fecal results
Uninfected untreated (UU)					
15325	0	0	0	0	neg
15328	0	0	0	0	neg
15330	0	0	0	0	neg
15331	0	0	0	0	neg
15332	0	0	0	0	neg
15333	0	0	0	0	neg
Infected untreated (IU)					
15318	32	29	7	12	pos
15319	7	12	1	2	pos
15320	13	9	0	14	pos
15321	0	0	0	0	neg
15322	16	16	0	5	neg
15323	2	2	0	2	pos
Infected untreated adults (IUA)					
15421	0	1	0	0	pos
15422	1	2	1	4	pos
15423	3	1	1	0	pos
15424	0	0	1	5	neg
15425	0	0	0	0	neg
15426	6	8	0	8	pos
Infected treated (IT)					
15334	0	0	0	0	neg
15335	0	0	0	0	neg
15336	0	0	0	0	neg
15338	0	0	0	0	neg
15339	0	0	0	0	neg
15341	0	0	0	0	neg

The number and sex identification of adult *T. cati* recovered in the intestine for each individual cat is recorded. If a cat had *T. cati* eggs identified on any of the weekly fecal examinations, a positive was recorded.

3.2. Analysis of CBC and BAL cytology

On serial peripheral blood CBCs, all cats in the infected groups (IU, IT, and IUA) developed an eosinophilia (>1000 μl^{-1}), which was significantly higher ($p < 0.05$) on day 36 than on day 0 or day 64. On day 64, a mild eosinophilia (1000–2500 μl^{-1}) was demonstrated in 2/6 IU cats and 2/6 IT cats and 0/6 IA cats. The eosinophilia appeared not to increase in response to the fourth and fifth infections. No significant changes in the total white blood cell count or absolute numbers of monocytes or lymphocytes were noted. The occasional cat did have basophils after infection. No cats had basophils present on CBC on day 64.

Most infected cats (5/6 IU, 5/6 IT, 4/6 IUA groups) had an eosinophilic cytology on BAL of greater than 50% at some point (day 36 or 64). The presence of >20% eosinophils on BAL was significantly present in all infected groups compared to UU cats and was significantly different in all infected groups from baseline on days 36 and 64 by paired *t*-test.

Eosinophilia of the BALs was assigned to the following grades: 0 = 1–16%, 1 = 17–35%, 2 = 36–60%, 3 = >60% (Table 2). Using a One Way ANOVA, a significant increase

Table 2
Bronchio-alveolar lavage cytology in cats: percent eosinophils.

Grade	Day 0 UU	Day 0 IU	Day 0 IT	Day 0 IUA	Day 35 UU	Day 35 IU	Day 35 IT	Day 35 IUA	Day 64 UU	Day 64 IU	Day 64 IT	Day 64 IUA
0	6	6	5	5	6	0	0	1	6	0	0	1
1	0	0	1	1	0	0	1	1	0	1	1	1
2	0	0	0	0	0	1	0	1	0	1	0	1
3	0	0	0	0	0	5	5	3	0	3	5	3

Percentage eosinophils on bronchio-alveolar lavage by grades: 0 = 1–16%, 1 = 17–35%, 2 = 36–60%, 3 = >60%. Listed as day of sampling after initial infection and as number of cats (6/group) in each group: Uninfected untreated (UU), infected untreated (IU), infected treated (IT), and infected untreated adult cats (IUA).

in the mean grade of eosinophilia found in the BAL fluid on day 64 was noted for all of the infected groups compared to the UU cats. There was not a significant difference ($p < 0.05$) between the infected groups. The IU group had the mean highest grade of eosinophilia on day 35, but the IUA group had the mean highest grade of eosinophilia on day 64. The IT cats had equal mean eosinophilia on BAL on day 36 and day 64. Using a Pearson Product Moment Correlation, there was only a weak correlation (correlation coefficient of 0.377) between the eosinophilia grade found on the BAL and the number of peripheral eosinophils on CBC.

3.3. Radiographic findings

The radiographic abnormality noted was primarily a bronchial pattern characterized by a peribronchial increase in density (Fig. 2A and B). At day 64, all infected kittens (6/6 in IU and 6/6 in IT) and most infected adults (4/6 in IUA) had bronchial–interstitial lesion scores of 1 or higher (0–3 scale) (Fig. 3). The radiographic scores for the infected cats in IU, IT, and IUA groups were significantly different ($p < 0.5$) on days 36 and 64 compared to their baseline on paired T testing. The average bronchial–interstitial score on day 64 for each group was 0 ± 0 for UU group, 1.9 ± 0.2 for UI, 1.5 ± 0.3 for IT, and 1.3 ± 0.5 for IUA. Radiographs on day 11 were not significantly different from their baseline in any group by paired T-testing, but 2 out of 6 in each infected group had bronchial scores of 1 and were abnormal. Enlarged pulmonary arteries were noted by a score of 1 (0–3 scale) in 0 of 6 cats in UU, 3 of 6 cats in IU, 3 of 6 cats in IT, and 4 of 6 cats in IUA group. The scoring of pulmonary arteries and radiographic pattern of the caudal lung lobes was indistinguishable from similar lesions in the early stages in feline heartworm (*Dirofilaria immitis*) disease. In all cats, bronchio-interstitial scores noted on day 64 were present at the same score or a higher score on day 36 radiographs.

3.4. CT and T. cati infections

3.4.1. High resolution computed tomography (HRCT) grades

On day 64, HRCT mean grade was 0.167 (SD 0.408) for UU cats, 2.167 (SD 0.753) for IU cats, and 1.667 (SD 1.033) for IT cats. In the IU and IT cats, HRCT mean grades were statistically different ($p < 0.05$) when compared with UU cats; however, a significant difference was not found

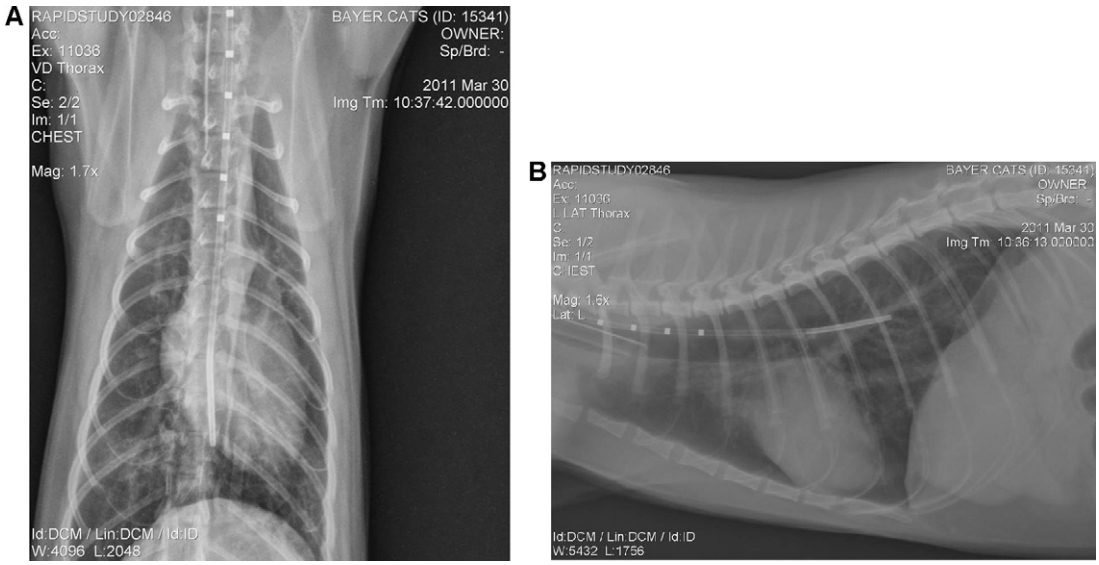

Fig. 2. (A) A ventro-dorsal radiograph of an infected cat. A ventro-dorsal radiograph demonstrates a diffuse increase in peribronchial densities most pronounced in the caudal lung lobes on day 64 in an infected untreated cat. This cat had 60% eosinophils on the cytology of the BAL fluid collected on day 64. (B) A Lateral Radiograph of an infected cat. A lateral radiograph demonstrates a diffuse increase in peribronchial densities most pronounced in the caudal lung lobes on day 64 in an infected untreated cat. This cat had 60% eosinophils on the cytology of the BAL fluid collected on day 64.

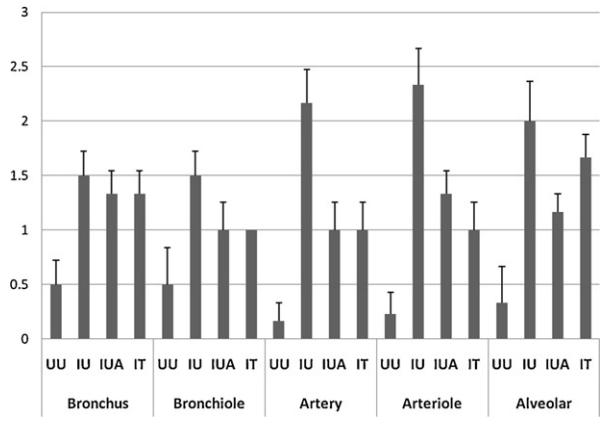

Fig. 3. Mean radiographic scores. Five different radiographic structures were scored (0–3, 3 = most severe; error bars = SD) in uninfected untreated cats (UU), infected untreated cats (IU), infected untreated adult cats (IUA), and infected treated cats (IT). All infected cats were significantly different from the UU cats in most diagnostic areas (see text).

between the IU and IT cats. All infected IU and IUA cats had some changes noted on day 11 compared with day 0 (Fig. 4). The lesions were randomly distributed within the same lung slice with linear striations in some areas. Evaluation of 1 mm sequential lung slices demonstrated areas of severe lung disease linearly adjacent to relatively normal areas. The evaluation of HRCT demonstrated that diseased areas did not conform to a predictable geometry or orientation relative to pulmonary arteries or airways. The reconstruction of 3D images of the lung surface confirmed the caudal lung lobe distribution in a non-predictable geometry (Fig. 5A and B).

3.4.2. Lung width

A statistically difference ($p > 0.05$) between day 0 and day 64 (percentage change of lung width) was found between the UU cats and all of the infected cats (IU, IT, and IUA). No difference ($p < 0.05$) was found in the percentage change of lung widths between the infected cat groups (Fig. 6). The UU cats' mean lung width increased over the 64 days of growth of the kittens by 3.68%. In contrast in the other infected kitten groups of same age, the lung width significantly decreased by 7.89% (IU cats) and 5.79% (IT cats).

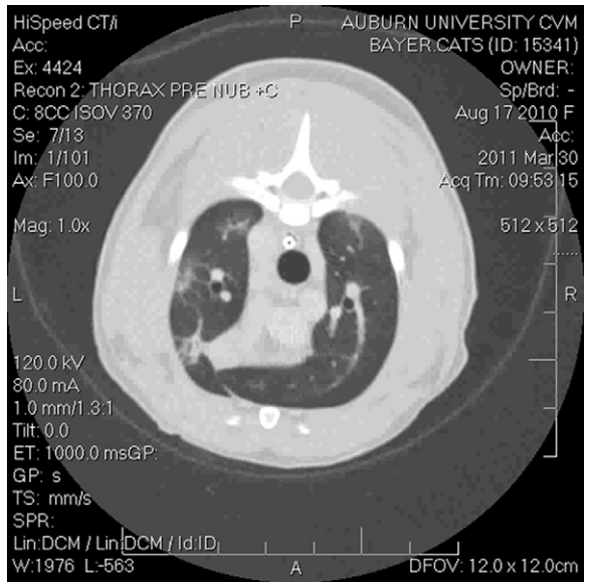

Fig. 4. CT Scan on cat on day 11 after infection. Example of 1-mm section just anterior to heart in an infected treated cat on day 11 after one oral infection with *T. cati*. The left lobe (left side of scan) was often the site of initial lesions, demonstrating increased densities of non-uniform distribution and geometry. Lesions may not be present in sections just 5 mm anterior or posterior. Involvement of lung adjacent to pleura was not uncommon and often areas adjacent to major pulmonary artery and bronchi would be normal as in this section. Radiographic changes on day 11 were uncommon, but subsequent radiographs on day 36 most often only revealed a diffuse bronchial pattern on VD and lateral views and the associated CT scan would demonstrate more significant disease.

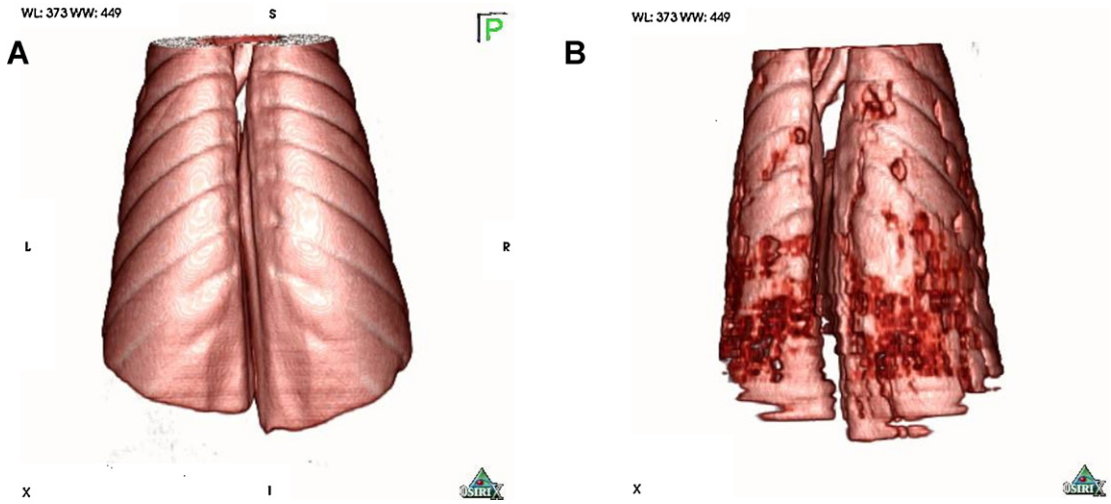

Fig. 5. (A) Three-dimensional reconstruction of CT scan at day 0. 3D reconstructions of sequential 1-mm slices from a fixed pressure inspiratory CT scan are depicted at day 0 in an infected untreated adult cat. No adult roundworms were recovered from the cat intestine. (B) Three-dimensional reconstruction of CT scan at day 64. 3D reconstructions of sequential 1-mm slices from a fixed pressure inspiratory CT scan are depicted at day 64 in an infected untreated adult cat. No adult roundworms were recovered from the cat intestine.

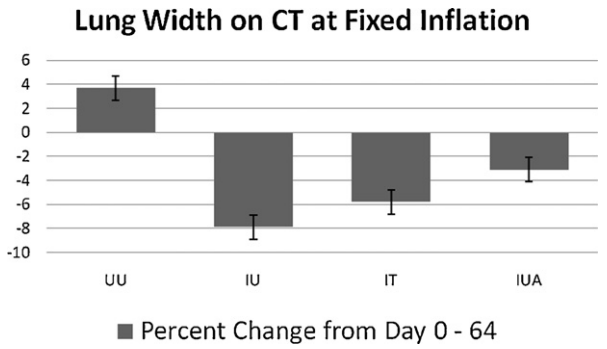

Fig. 6. Lung width in cats infected with *T. cati*. Each cat had the lung width measure at a fixed anatomical site at day 0 and at day 64 and expressed as a percentage change from baseline. In uninfected untreated cats (UU) the lung width increased, as compared to the decrease in age matched infected untreated cats (IU) and infected treated cats (IT), and also in infected adult cats (IUA).

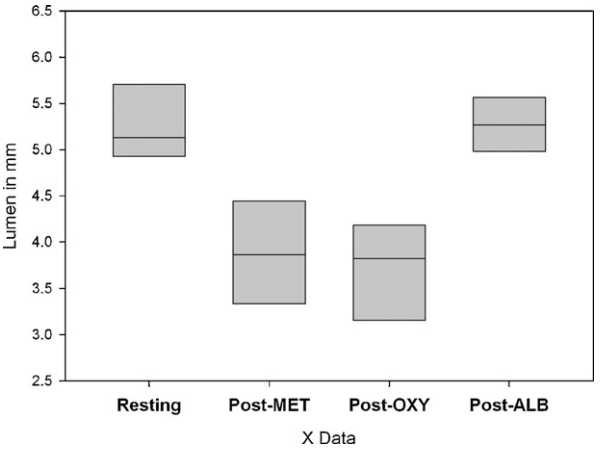

Fig. 7. Bronchial ring in vivo reactivity. Bronchial ring diameter was measured on a 1-mm section of CT scan in uninfected untreated (UU) cats comparing resting, post-methacholine nebulization for 2 min (post-MET), post-oxygen ventilation for 5 min (post-OXY), and post-albuterol nebulization for 2 min (post-ALB).

In the IUA cats, the lung width also significantly decreased ($p < 0.05$) over time by 3.09%.

3.4.3. *In vivo bronchial reactivity*

Evaluation of the percentage change before and after methacholine or albuterol nebulization by calculation of total lumen cross-sectional area vs. direct measure of cross-sectional lumen diameter revealed no statistical difference. Thus, the bronchial diameter data were used for statistical analysis. The lumen size before and after the nebulization of methacholine were highly significantly different on the day 0 (24 cats) ($p < 0.001$). After methacholine nebulization in UU, IT, and IU cats with a fixed pressure of 14 cm H_2O, the average mean diameter bronchi lumen decreased from 4.89 to 4.22 mm. The mean percentage decrease in lumen diameter was 13.789% (SD ± 3.129, SEM ± 0.863).

At day 0 (24 cats) the lumen size after nebulization of albuterol compared to lumen size after the nebulization of methacholine very significantly increased ($p < 0.001$) from 4.225 to 4.909 mm with the mean percentage increase in lumen of 18.7% (SD 8.8, SEM 3.83). Using a paired *t*-test on the day 0 values for the 24 cats, a significant difference was not found when baseline lumen size day 0 baseline data (i.e. before nebulization of methacholine) was compared to post treatment data (i.e. nebulization of albuterol). No difference in percentage decrease of lumen size on day 64 after the nebulization of methacholine was noted between any group of cats (UU cats 14.7%, the IU cats 3.1%, the IT cats 10.033%, and the IUA cats 19.022%).

In the UU group on day 64, the effect of oxygen alone for 5 min had no effect on methacholine induced contraction of the bronchus and bronchiodilation was then demonstrated by albuterol nebulization (Fig. 7).

3.4.4. *HRCT lung density frequency*

Analysis of the baseline HRCT density frequency for the 24 cats demonstrated repeatable curves with minimal standard deviations in the calculated values (Fig. 8A). A significant difference ($p < 0.05$) was noted in the frequency of pixels at −600, −856, −910, −925, and −950 comparing normal values from the UU cats and both the IU and IT groups on day 64 (Fig. 8B). A significant difference in the frequency of pixels at −600 and −856 was found between the UU and IUA adult cats. A significant difference in the frequency of pixels found at −600, −856, −910, and −925 was found between the UU and IT cats (Fig. 9A and B).

A significant difference in pixels was not found at −950, −925, or −910 between the UU and IUA cats or at −950 between the UU and IT cats. At the above cut-off values of −600 and −856 no difference was noted between IU and IUC cats or between IU and IT cats. In the frequency distribution curve, the shift in the curve to the right reflected change over time (Fig. 8B), was associated with a decrease in air densities (−925), and an increase in tissue densities (−800 to −600).

3.5. *Necropsy findings*

On gross examination, the lungs of the infected cat groups (6/6 IT, 6/6 IU, and 5/6 IUA cats) had randomly distributed small depressed lesions (Fig. 10). Lung abnormality was grossly more apparent after fixed pressure perfusion. None of the UU cats had any gross abnormality of the lung. No gross abnormalities were noted in any cats in the heart, kidney, bronchial lymph nodes, or liver. Adjacent to surface lesions on the lung, the parietal surface of the pleura and the surface of the diaphragm appeared to be normal.

3.6. *Histopathology*

3.6.1. *Lung pathology*

The bronchus, bronchiole, pulmonary artery, pulmonary arteriole, and alveolar/interstitial areas were scored 0–3 (Fig. 11). All infected groups (IU, IT, IUA) had statistically higher scores ($p > 0.05$) than uninfected cats (UU) in each variable scored. The IT cats had significantly ($p < 0.05$) lower pulmonary artery, arteriole, and bronchiole histopathologic scores than the IU cats. The IUA cats had significantly ($p < 0.05$) lower artery and arteriole scores than the IU kittens. The alveolar–interstitial scores were

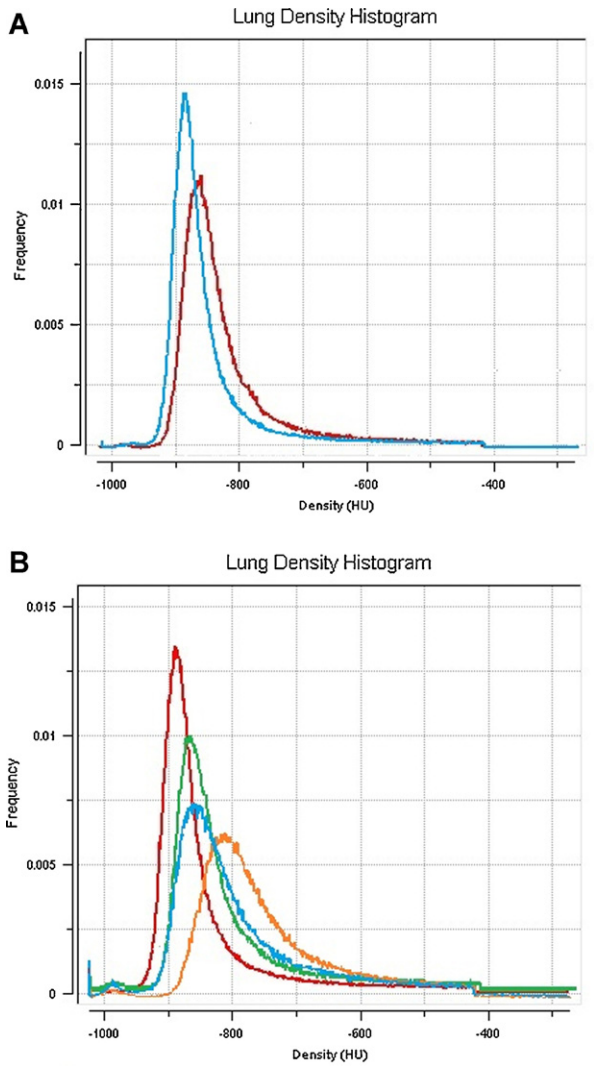

Fig. 8. (A) Density curve of Hounsfield units on inflation lung CT scan in an uninfected untreated cat. With software masking of solid organs, the average of sequential 1-mm slices of the entire lung was evaluated. An uninfected untreated cat was scanned on day 0 (red line) and compared to day 64 (blue line) reflecting a non-significant shift associated with growth. (B) Density curve of Hounsfield units on inflation lung CT scan in a *Toxocara cati* infected treated cat. With software masking of solid organs, the average of sequential 1-mm slices of the entire lung were evaluated. A *T. cati*-infected treated cat was scanned on day 0 (red line), day 11 (green line), day 36 (orange line), and day 64 (blue line). The cat in B had no adult worms recovered from intestine. A shift toward the right illustrates increased opacity. A shift toward the left, not observed, is typical of air trapping.

consistently higher than the bronchial scores in infected cats in all groups. Evaluation of the interstitium revealed a marked increase in fibroblasts in all infected cats in all groups with a noted prominence of the alveolar struts (Fig. 12A and B). The smooth muscle actin stain demonstrated more significant increases in the smooth muscle of the pulmonary arteriole than in the bronchioles in infected cats. Infected cats had random increased actin-stained myofibroblasts in the interstitial parenchymal and alveolar struts. The actin staining interstitial myofibroblasts

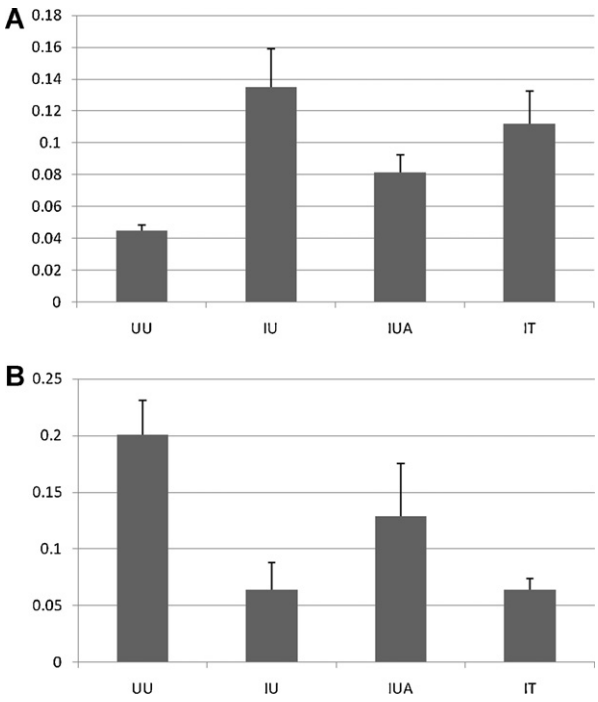

Fig. 9. (A and B) Changes in specific Hounsfield units on CT scans. Significant differences ($p < 0.001$) were noted between infected cat groups (IU, IUA, and IT) and uninfected untreated cats (UU) at the −600 (A) and −856 (B) Hounsfield units.

were distributed unassociated with either the pulmonary vasculature or the airways (Fig. 13A–D). In cats with lung disease, no larvae or fragments were identified in lung tissue. In the UU cats, no lung pathology was identified that resulted from the repeated diagnostic procedures.

3.6.2. Morphometry of pulmonary arteries and bronchus

In the morphometry of the walls of the pulmonary arteries, all of the infected groups demonstrated an increase in the lumen/wall ratio. The lumen-to-wall ratio was

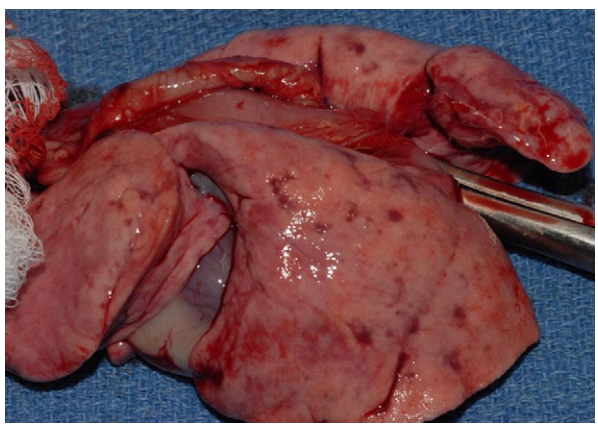

Fig. 10. Cat lung on day 65 after *T. cati* infection. Example of the gross examination of the lung of an infected untreated cat that had been infected with serial oral doses of *T. cati* infective eggs. Surface demonstrates multiple punctuate non-uniform lesions.

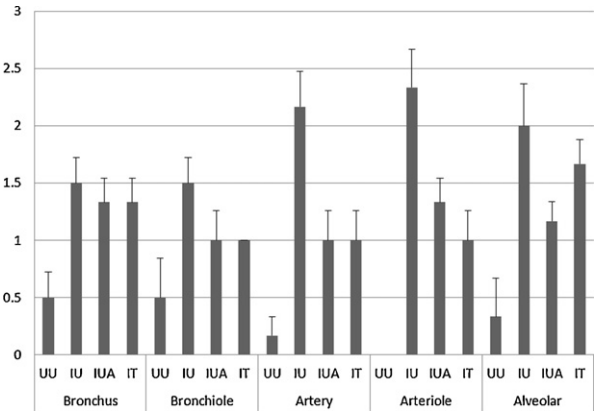

Fig. 11. Mean histopathologic scores of lung. Five different areas of lung H&E were scored (0–3, 3 = most severe; error bars = SD) in uninfected untreated cats (UU), infected untreated cats (IU), infected untreated adults (IUA), and infected treated cats (IT). Most variables in IU, IUA, and IT cats were significantly different from UU cats. None of the infected groups were significantly different from each other (see text).

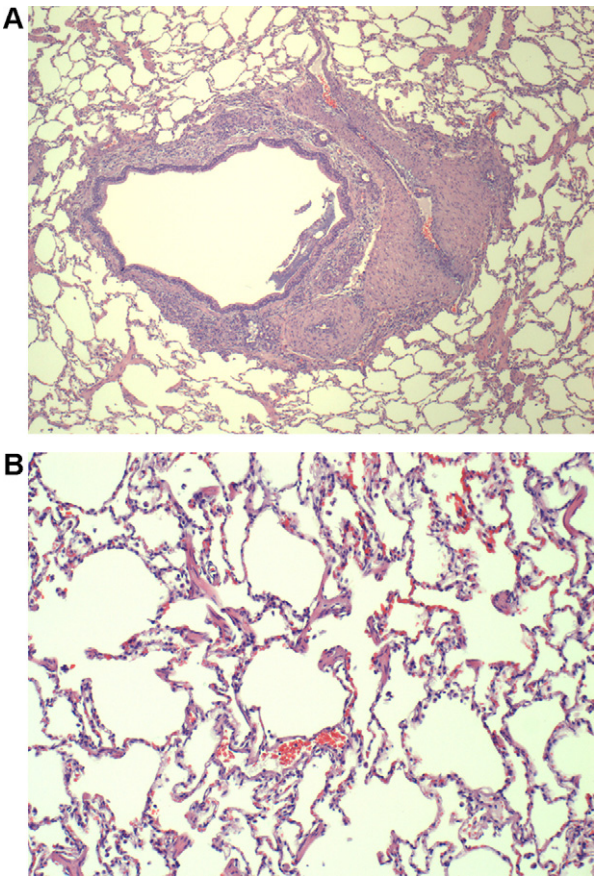

Fig. 12. (A and B) Histopathology of cats. Fixed pressure perfused lung was sectioned for H&E staining. The disease was not uniformly distributed, but most infected cats after examination demonstrated pulmonary artery intimal and smooth muscle hyperplasia at times that was also associated with bronchial disease (A), but often diffuse smooth muscle proliferation was randomly noted in the interstitial areas (B).

significantly ($p > 0.05$) decreased in the IU group compared to IT cats. Despite abnormal bronchus on light microscopic grading, the lumen/wall ratios of the airways were not statistically different between groups (Fig. 14A and B).

3.6.3. Histopathology of liver

No liver abnormalities were observed by light microscopy on liver sections in any of the cats.

3.7. In vitro bronchial ring reactivity

There were no significant differences in intrapulmonary bronchiole (IPB) dimensions (length, weight, circumference, or wall thickness) between infected groups and UU cats. There were no significant differences in maximum active force after contraction to 10^{-5} M ACh. IPB from IU and UU cats had concentration dependent contractile responses to ACh and to 5-HT. There were no significant differences in responses to ACH or 5-HT between IU and UU cats (Fig. 15A and B). IPB from IU cats had a significantly increased response to histamine (Fig. 15C). The AUC for histamine was significantly increased in IU vs. UU cats ($p = 0.0168$).

In evaluation of relaxation responses, there were no significant differences between groups (Fig. 15D). Rings from IU and UU groups relaxed maximally approximately 45% to SNP and 20% to SubP (Fig. 15E and F) and there were no differences between groups for isoproterenol (ISO), sodium nitroprusside (SNP) or substance P (SubP).

4. Discussion

Marked lung disease was induced by the oral administration of *T. cati* L3 in both kittens and adult cats that would be clinically detected by BAL, thoracic radiographs, or CT scan. Importantly, the abnormalities were noted in cats that did not develop intestinal parasites (1/6 infected kittens, 2/6 infected adults, and 6/6 infected cats on preventative medication). Based on the CT density, pulmonary arterial morphometry and histopathologic scores, kittens on preventive medication did have some statistical attenuation of lesions, but these differences were of very limited clinical relevance. In a clinical setting, association of the lung disease with a recent infection with *T. cati* would be difficult as in the present study of cats that had negative fecal examinations (2/6 infected kittens, 2/6 infected adults, and all 6/6 infected treated cats); all of which had predominant eosinophilic cytology on BAL, and lung lesion based on radiographs and CT scans. The dose of *T. cati* was based on prior laboratory challenges (Swerczek et al., 1970) and may be higher than client owned cats may acquire, but this proof of concept study demonstrates that *T. cati* induced lung disease should be included in the differential diagnosis of cats with a bronchial pattern or enlarged pulmonary arteries on radiographs. The dose in the adult cats was lower and closer to efficacy trials (Jacobs et al., 1994) but the lung disease was, on diagnostic evaluation, just as severe as the higher dose in kittens and identified after a single infective dose.

The timing of the changes relative to infection appears to be rapid. The lesions in cats in all infected groups were

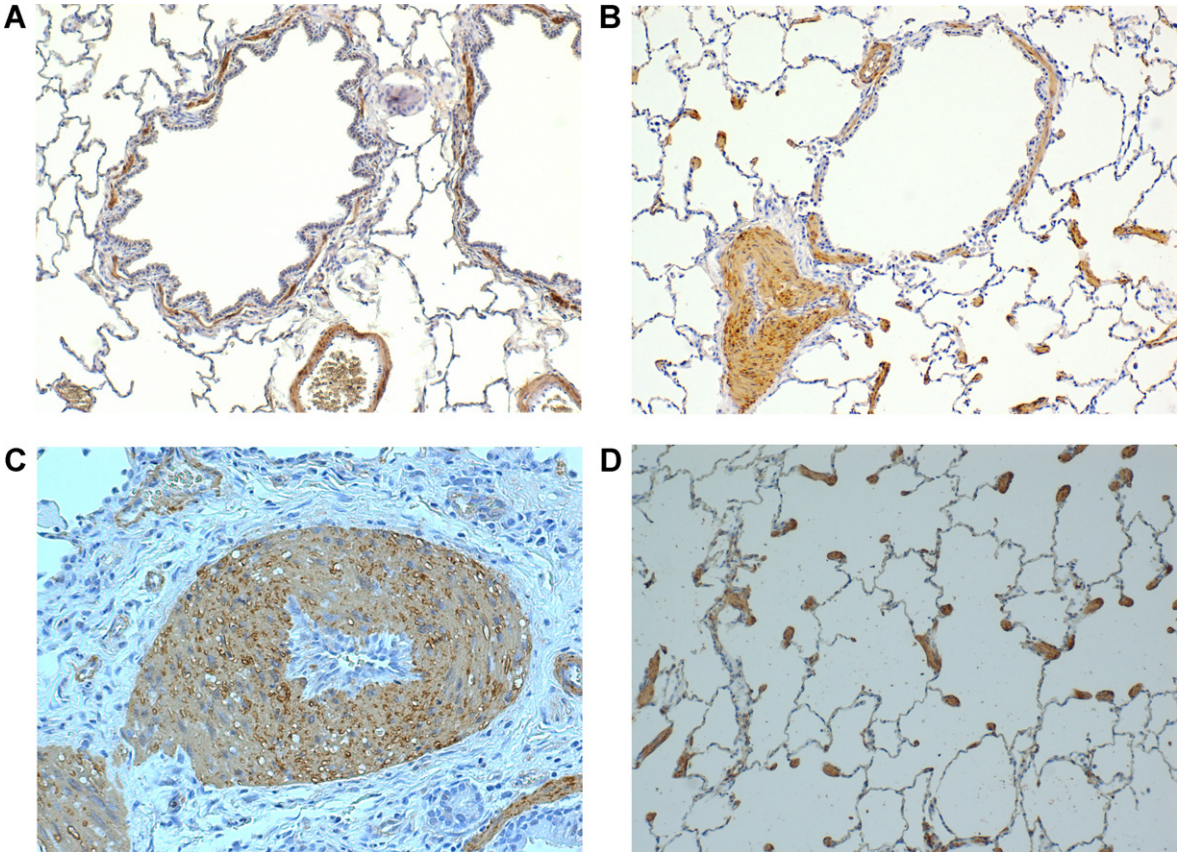

Fig. 13. (A–D) Histopathology with alpha-smooth muscle actin staining. Fixed pressure perfused lung was sectioned for smooth muscle actin staining. The uninfected untreated cats (A, 10×) were compared to infected cats. The pulmonary artery smooth muscle proliferation could be associated with relatively normal airways (B, 10×). The pulmonary arterial changes were often severe (C, 20×), but consistent changes included smooth muscle proliferation and prominent alveolar struts (D, 20×).

noted on the first CT performed on day 11 and thus were the result of a single oral dose of *T. cati*, as the second L3 dose was administered on day 11 after the CT scan. Experimental *T. canis* infections in dogs (Schnieder et al., 2011) found *T canis* larvae migrating in the lung by day 3 after infection, which suggests that performing a CT in cats before day 11 may have demonstrated earlier lesions in infected cats. The relationship between the early involvement of CT densities most often noted in the caudal portion of right anterior lung lobe on day 11 and the migration pattern of *T. cati* larvae is unexplained. Also unclear is the pathogenesis of the lesions of the pleural margins related to larvae maturation in the lung. If *T. cati* is transported via blood flow from the liver via post-cava to right ventricle, the distribution of CT changes would be supportive as most severe lesions by days 34 and 64 were in the caudal lung lobes (Fig. 5A and B).

The random pattern of the lesions is focal patches of linear densities adjacent to relatively normal lung. The radiographic pattern of the lung lesions in the present study is similar to those of feline heartworm disease, but feline heartworm disease is associated with a significant peribronchial disease and the failure of airways to bronchial constrict or bronchial dilate (Wooldridge et al., 2012). Using the same methodologies, the present study showed the airways of cats with *T. cati* continue to demonstrate a normal response to stimuli, and not a blunted response as in heartworms, or an exaggerated response as would be expected in a hyper-reactive airway, as in asthma. Further, the histologic lesions in *T. cati* infected cats, while significant in the pulmonary arteries and interstitial areas, were relatively mild around the bronchioles when compared to the bronchial disease of feline heartworm infection. The interstitial smooth muscle proliferation demonstrated in *T. cati*-infected cats appeared to be independent of direct extension from either the pulmonary artery hypertrophy or bronchial areas. The interstitial pattern of disease is not uniform throughout the lung lobes, as demonstrated by the uneven distribution on sequential CT slices and patchy honeycombed appearance. Examination of sequential histopathology slides from the corresponding tissue block also confirmed the random distribution of interstitial lung lesions and a non-linear pattern of pulmonary arterial disease. Even in the same lung slice, areas of airway and pulmonary arterial disease could exist in the same slice as normal structures. These data suggest that histopathologic evaluation of a single lung section in random sourced cats is of very limited accuracy in identifying the nature of widely distributed but randomly focal areas of disease. Looking at the correlation coefficients for the various diagnostic modalities, the typical “bronchial pattern” described on

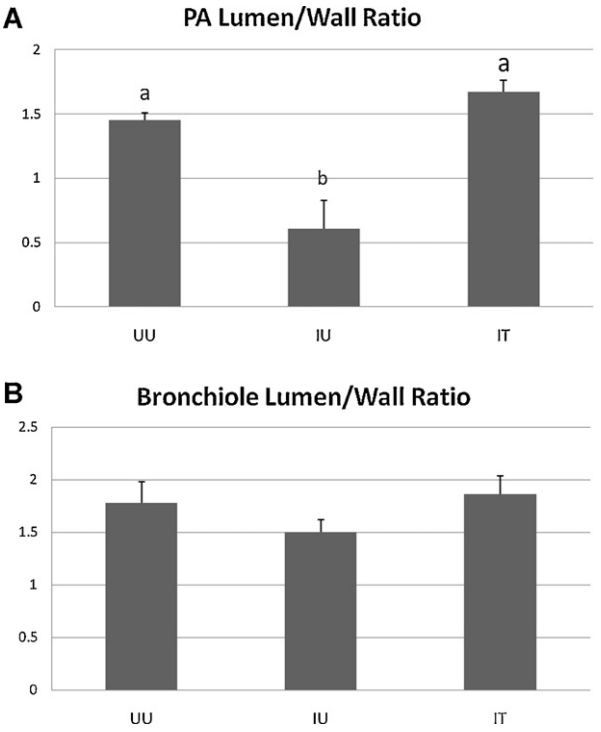

Fig. 14. (A and B) Lumen-to-wall ratios for pulmonary artery and bronchiole. The ratio of the area of the lumen to wall was calculated for each cat based on multiple measures of the pulmonary arteries (A) and airways (B) on lung histopathogy. For the pulmonary artery, the infected treated cats (IT) were not significantly different from the uninfected untreated cats (UU), and both were significantly different from thickened arterial walls of infected untreated cats (IU). There was no significant difference between any of the groups on bronchial way thickness. Superscripts are different from each other ($p < 0.05$).

radiographs was more closely associated with an increase in the CT and histopathologic interstitial markings that may not be immediately peribronchial. (Table 3). The present study demonstrates that statistical evaluation of morphometric data of pulmonary artery or airway lumen/wall ratios from one section of lung would have limitations in characterization of random disease processes.

Although the peripherial eosinophilia was moderate and transient in all infected cats, 5/6 cats in all infected groups demonstrated greater than 60% eosinophilia on cytology of the BAL fluid on at least day 35 or day 64 of the study. Further most infected cats had eosinophilia on cytology of BAL fluid (>16 on day 11) after a single infection of *T. cati*. Normal bronchial reactivity by both in vitro (days 11, 36, and 64) and in vivo challenge (day 64) was demonstrated in cats with consistent eosinophilia on BAL examination. These findings combined with the radiographic changes classically described as a bronchial lung pattern are of clinical significance in the evaluation of client owned cats. An oral infection with *T. cati* induced a clinical diagnostic profile indistinguishable from that typically associated with hyper-responsive airway disease ("asthma") and from the hyporeactive airways of feline heartworm disease. Further, T. *cati* infection may induce a lung disease which provides a background of diagnostic abnormalities which may be present in asymptomatic cats. The repeated exposure of cats over time to oral *T. cati* may induce a different airway response to challenge. Nebulization of methocholine as a provocative challenge during CT scans may have utility in differentiating airway responsiveness in cats presented for coughing or dyspnea.

The collection of serial CT scan data for 3D reconstruction and evaluation of serial transections of the lung was key to identifying the uneven distribution of lung pathology that cannot be discerned in radiography. The attempts to calculate changes in density on simple sequential (three to five 1-mm sections, or three 5-mm sections) in carefully defined regions of interest were unsuccessful. The random distribution of focal patchy lesions precluded success with this methodology. By inflating the lung to a fixed pressure and sequentially averaging all the slices with a masking technique, the density distribution (amount of air vs. various tissue densities) correlated with histologic findings. This method for the extraction of the lung mask is comparable to other methods (Hu et al., 2001). No attempt was made to exclude airways from the mask and, therefore, from the density mask analysis (Hersh et al., 2007).

Based on these analyses, the significant increases in the −600 HU and −825 HU densities in infected cats represented an increase in interstitial parenchyma in the lung. Air trapping as in asthma or emphysema would have resulted in an increase at the other end of the spectrum above −925 HU (left side of Fig. 8B). With the increased accessibility of CT for client cats, these methods may find value in determining interstitial vs. bronchial disease vs.

Table 3
Correlation of different diagnostic evaluations of cats infected with *T. cati*.

Histopathology correlation coefficients to HRCT and radiographic grading					
	Histopathology				
	Bronchus	Bronchiole	Artery	Arteriole	Alveolar
HRCT grade correlation coefficient	0.714	0.528	0.775	0.701	0.854
p-Value	<0.001	0.0244	<0.001	0.0012	<0.001
Bronchio-interstitial coefficient	0.655	Weak	0.689	0.795	0.783
p-Value	0.00319		0.00158	<0.001	<0.001
Bronchial coefficient	0.592	Weak	Weak	0.509	0.57
p-Value	0.00963			0.0309	0.0136
Interstitial coefficient	0.587	Weak	0.718	0.827	0.764
p-Value	0.0105		<0.001	<0.001	<0.001
Parts coefficient	None	Weak	0.514	Weak	Weak
p-Value			0.0291		

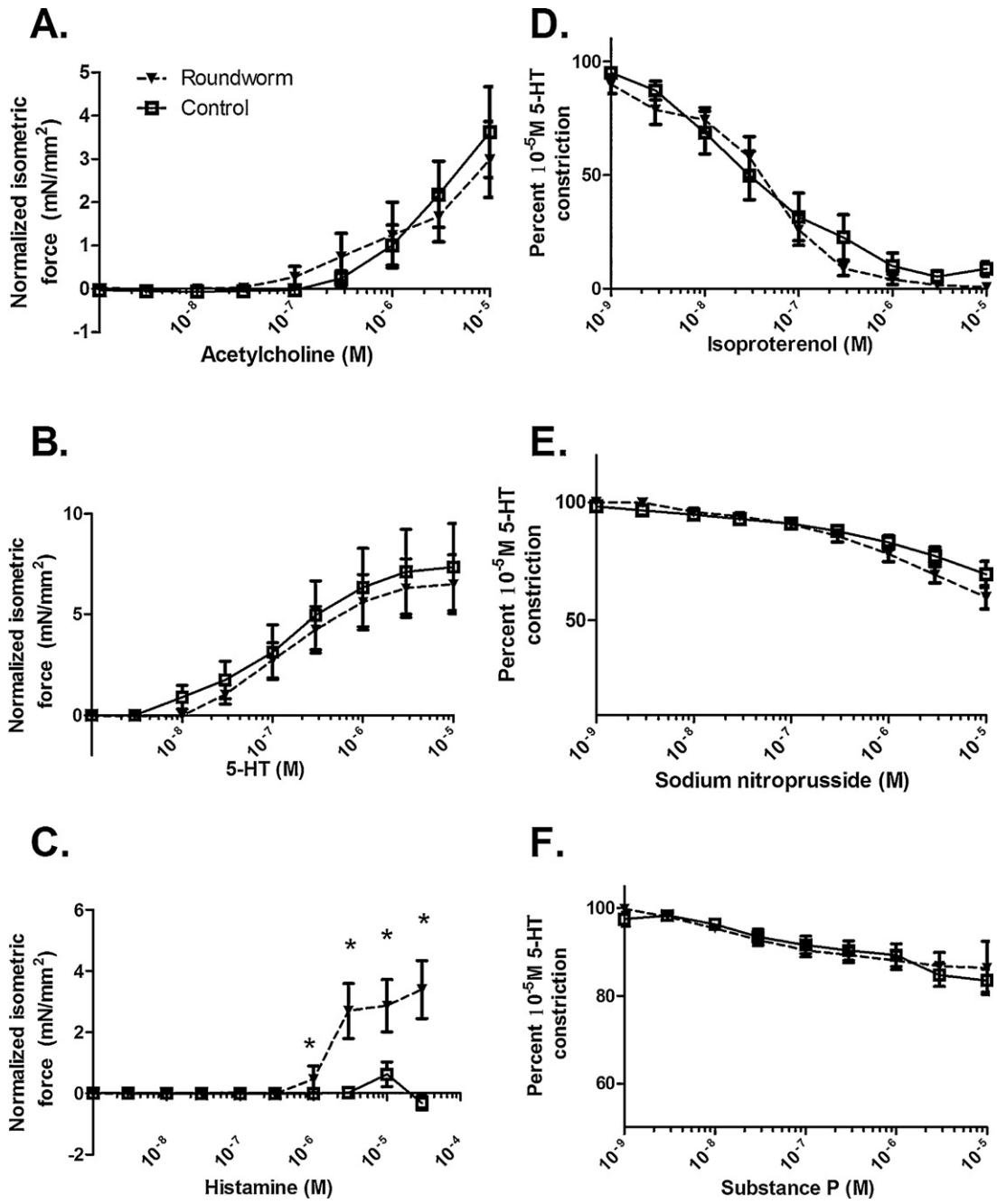

Fig. 15. In vitro bronchial ring reactivity. This figure shows the effect of roundworm infection on contractile and relaxation responses of feline intrapulmonary bronchioles (IBPs). All contractile responses are expressed as normalized isometric force, which is calculated as the active force (maximum-baseline) divided by the CSA of the ring and all relaxation responses are expressed as a percentage of the force elicited by 5-hydroxytryptamine (5-HT). (A and B) Contractile responses to ACH and 5-HT are not different in rings from roundworm vs. control cats. (C) IPBs from roundworm-infected cats have an increased contractile response to HIS. (D–F) There are no differences in relaxation responses between groups. Acetylcholine (ACH), histamine (HIS), isoproterenol (ISO), sodium nitroprusside (SNP), substance P (SubP). IPB (–▼–) from roundworm infected cats, IPB (–□–) from control cats. $^{*}p < 0.05$.

hyper-reactive airway disease and have utility in research where sequential 3 dimensional studies of the same animal would replace multiple study groups.

The measurement of the lung diameter on CT scans at a fixed pressure further supports the interstitial component of *T. cati* induced lung pathology (Fig. 6). Normal unaffected growing kittens had their chest cavity increase by 3.7% over two months. But the chest cavity diameter decreased in age matched infected untreated kittens (7.89%) and also in infected cats on preventive medications (5.78%), which illustrates the limited attenuation of lung pathology by preventative medication. Of note, the adult cats, assuming no

growth, also had decrease in chest diameter by 3.09% after infection compared to baseline. The decrease in expansion of the chest wall at a fixed pressure and the increase in lung CT densities at −600 HU suggest that the interstitial disease induced by *T. cati* larval migration is a restrictive interstitial disease. Whether the lung pathology becomes more severe and results in a decrease in total tidal volume with repeated exposures over a cat's life is of clinical significance, as is the question as to whether these lesions of the interstitium and pulmonary arteries are reversible.

The unique smooth muscle proliferation noted in *T. cati* infected cats was structurally independent of pulmonary artery and bronchial changes. Cats, but not dogs, have pulmonary intravascular macrophages (PIMs) (Dillon et al., 2008). PIMs reside permanently attached to the pulmonary capillary endothelial surface and have open channels with the associated endothelial cell. The PIMs' positioning and macrophage function may modulate the host response to a larva sharing the same capillary bed. Based on early work (Sprent, 1956) with oral infection of *T. cati* eggs in cats, the distribution of the larvae in the lungs was highest in number from days 6 to 21 after oral infection and the larvae were 0.36–0.45 mm in size. The size of the larvae precludes passage through the pulmonary capillary bed. In cats with adult live heartworms, an adaptive or induced down regulation of PIM phagocytic activity was noted (Dillon et al., 2008). The rapid arrival of *T. cati* L3 after oral infection in cats would preclude the ability of the parasite to modulate the PIM activity unless there is an inherent production by the parasite of a substance with this capacity. In the present study, the increased CT densities noted on the CT on day 35 in many cats were more severe than on day 64 and could reflect an inflammatory disease that had resolved by day 64.

The clinical implications of this study are concerning. The oral infection of a domestic owned cat with *T. cati* already on preventive medication, or even infection of adult cats, may result in lung disease without the development of intestinal stages. The resultant lung changes may become background pathology that will be present on diagnostic testing of even asymptomatic cats. In the present study, the last infective dose was on day 43, but all cats in the infected groups at day 64 had an eosinophilic cytology on BAL fluid analysis, a radiographic peribronchial diffuse pattern, and many had mildly enlarged caudal pulmonary arteries on thoracic radiographs. This diagnostic pattern cannot be differentiated from that of feline heartworm disease or *Aelurostrongylus* infection and other non-specific lung diseases of cats. These cats were closely monitored and no immediate clinical signs were noted, however the cats were sedated for all procedures and had minimal activity. The absence of clinical signs in the cats of the present study does not predict the long term consequences of the lung disease, or the pulmonary response to subsequent infections over time.

The ability of this parasite in the cat to migrate rapidly through the lung is central to the challenge of preventing lung disease with medication. Examination of the liver in infected treated cats did not note any areas of inflammation or granulomas, which might have been anticipated if the moxidectin/imidacloprid combination had abated the parasites' survival through the liver. This study was designed to replicate exposure of client cats already on preventive medication when infected. The lung disease was statistically attenuated by pre-treatment with two doses (at day −55 and day −25) of this specific preventive medication, but the site of the action is unclear. Whether pre-treatment for a longer period with moxidectin/imidacloprid or use of a different preventative medication has the ability to prevent lung migration after *T. cati* oral infection is unknown. Regardless, after oral ingestion of *T. cati*, lung disease which alters BAL cytology and radiographic interpretation developed quickly in cats already on this specific preventative medication and the lung disease was not significantly influenced by whether adult intestinal stages develop.

5. Conclusion

For cat owners and the veterinary profession, these data are very concerning. The prevention of internal parasites has been a core responsibility of veterinary practice. These data suggest that despite the profession's best intent, while the prevention of the development of adult parasites after oral exposure to *T. cati* is obviously beneficial, this practice even with good client compliance will not prevent the development of lung disease. Medications that prevent adult *T. cati* from developing will stop egg shedding, which, based on this study, is the central risk factor for all cats. The clinical consequence of repeated infections over time and compounding lung disease is unknown. Regardless of this, the *T. cati*-induced disease can induce a bronchial pattern and enlarged pulmonary arteries on thoracic radiographs, an eosinophilic cytology on BAL with normal bronchial reactivity, and honeycombed pattern of increased densities on thoracic CT. The HRCT scan represents an important research tool and has clinical applications in investigating lung disease and in vivo bronchial reactivity. The lung disease of *T. cati* is independent of the development of adult parasites and cannot be ruled out by a negative fecal examination, age of the cat, or a history of preventive medication.

Funding source

Bayer Healthcare LLC, Animal Division, Shawnee Mission, Kansas; Auburn University Cardiovascular Laboratory (A.R. Dillon). Bayer Healthcare, Animal Division was involved in experimental study design, but was not involved in data collection or statistical evaluation.

Conflict of interest statement

The PI on this study has had confidentiality agreements and/or served on Scientific Advisory Boards with Bayer Healthcare LLC, Pfizer Animal Health, Merial Inc., Idexx Laboratories, Elanco Animal Health, Medtronic Inc. Medical Device Division.

References

Arther, R.G., Charles, S., Ciszewski, D.K., Davis, W.L., Settje, T.S., 2005. Imidacloprid/moxidectin topical solution for the prevention of heartworm disease and the treatment and control of flea and intestinal nematodes of cats. Vet. Parasitol. 133, 219–225.

Blagburn, B., 2010. Where have all the parasites gone? Results of national parasite and vector-borne diseases survey? In: Novartis Parasite Symposium, NAVC.

Blagburn, B.L., Lindsay, D.S., Vaughan, J.L., Rippey, N.S., Wright, J.C., Lynn, R.C., Kelch, W.J., Ritchie, G.C., Hepler, D.I., 1996. Prevalence of canine parasites based on fecal floatation. Compend. Cont. Ed. Pract. Vet. 18, 483–509.

Borthakar, S.K., Mukharjee, S.N., 2011. Gastrointestinal helminthes in stray cats (*Felis catus*) from Aizawl, Mizoram, India. J. Trop. Med. Pub. Health 42 (2), 255–258.

Bowman, D.D., 2009. Georgis' Parasitology for Veterinarians, 9th ed. WB Saunders, Philadelphia, 451 pp.

Coati, N., Schnieder, T., Epe, C., 2004. Vertical transmission of *Toxocara cati* Schrank 1788 (Anisakidae) in the cat. Parasitol. Res. 92, 142–146.

Companion Animal Parasite Council, 2012. Recommendations for Intestinal Parasites: Ascarids, Hookworms, Whipworms, Giardia, Coccidia. http://www.capcvet.org (retrieved 05.01.12).

DeSantis, A.C., Raghavan, M., Caldanaro, R.J., Glickman, N.W., Moore, G.E., Lewis, H.B., Schantz, P.M., Glickman, L.T., 2006. Estimated prevalence of nematode parasitism among pet cats in the United States. J. Am. Vet. Med. Assoc. 228, 885–892.

Dillon, A.R., Warner, A.E., Brawner, W., Hudson, J., Tillson, M., 2008. Activity of pulmonary intravascular macrophages in cats and dogs with and without adult *Dirofilaria immitis*. Vet. Parasitol. 158, 171–176.

Epe, C., 2009. Intestinal nematodes: biology and control. Vet. Clin. North Am. Small Anim. Pract. 39, 1091–1107.

European Scientific Counsel Companion Animal Parasites, 2006, December. Worm Control in Dogs and Cats. Guideline 1. http://www.esccap.org

Fahrion, A.S., Schnyder, M., Wichert, B., Deplazes, P., 2011. Toxocara eggs shed by dogs and cats and their molecular and morphometric species-specific identification: is the finding of *T. cati* eggs shed by dogs of epidemiological relevance? Vet. Parasitol. 177, 186–189.

Gates, M.C., Nolan, T.J., 2009. Endoparasite prevalence and recurrence across different age groups of dogs and cats. Vet. Parasitol. 166, 153–158.

Hersh, C.P., Washko, G.R., Jacobson, F.L., Gill, R., Estepar, R.S., Reilly, J.J., Silverman, E.K., 2007. Interobserver variability in the determination of upper lobe-predominant emphysema. Chest 131, 424–431.

Hu, S., Hoffman, E.A., Reinhardt, J.M., 2001. Automatic lung segmentation for accurate quantitation of volumetric X-ray CT images. IEEE Trans. Med. Imaging 20, 490–498.

Jacobs, D.E., Arakawa, A., Courtney, C.H., Gemmell, M.A., McCall, J.W., Myers, G.H., Vanparijs, O., 1994. World Association for the Advancement of Veterinary Parasitology (W.A.A.V.P.) guidelines for evaluating the efficacy of anthelmintics for dogs and cats. Vet. Parasitol. 52, 179–202.

Johnson, V.S., Corcoran, B.M., Wotton, P.R., Schwarz, T., Sullivan, M., 2005. Thoracic high-resolution computed tomographic findings in dogs with canine idiopathic pulmonary fibrosis. J. Small Anim. Pract. 46, 381–388.

Johnson, V.S., Ramsey, I.K., Thompson, H., Cave, T.A., Barr, F.J., Rudorf, H., Williams, A., Sullivan, M., 2004. Thoracic high-resolution computed tomography in the diagnosis of metastatic carcinoma. J. Small Anim. Pract. 45, 134–143.

Little, S., 2011. Customized approach to parasite control: risk assessment and routine deworming of pets. In: Bayer Symposium Series, 2011 Cutting-Edge Proceedings NAVC Experience.

Little, S.E., Johnson, E.M., Lewis, D., Jaklitsch, R.P., Payton, M.E., Blagburn, B.L., Bowman, D.D., Moroff, S., Tams, T., Rich, L., Aucoin, D., 2009. Prevalence of intestinal parasites in pet dogs in the United States. Vet. Parasitol. 166, 144–152.

Macuhova, K., Kumagai, T., Akao, N., Ohta, N., 2010. Loop-mediated isothermal amplification assay for detection and discrimination of *Toxocara canis* and *Toxocara cati* eggs directly from sand samples. J. Parasitol. 96, 1224–1227.

Martínez-Barbabosa, I., Vázquez Tsuji, O., Cabello, R.R., Cárdenas, E.M., Chasin, O.A., 2003. The prevalence of *Toxocara cati* in domestic cats in Mexico City. Vet. Parasitol. 114, 43–49.

McTier, T.L., Shanks, D.J., Wren, J.A., Six, R.H., Bowman, D.D., McCall, J.W., Pengo, G., Genchi, C., Smothers, C.D., Rowan, T.G., Jernigan, A.D., 2000. Efficacy of selamectin against experimentally induced and naturally acquired infections of *Toxocara cati* and *Ancylostoma tubaeforme* in cats. Vet. Parasitol. 91, 311–319.

Mircean, V., Titilincu, A., Vasile, C., 2010. Prevalence of endoparasites in household cat (*Felis catus*) populations from Transylvania (Romania) and association with risk factors. Vet. Parasitol. 171, 163–166.

Nolan, T.J., Smith, G., 1995. Time series analysis of the prevalence of endoparasitic infections in cats and dogs presented to a veterinary teaching hospital. Vet. Parasitol. 59, 87–96.

Nutter, F.B., Dubey, J.P., Levine, J.F., Breitschwerdt, E.B., Ford, R.B., Stoskopf, M.K., 2004. Seroprevalences of antibodies against *Bartonella henselae* and *Toxoplasma gondii* and fecal shedding of *Cryptosporidium* spp., *Giardia* spp., and *Toxocara cati* in feral and pet domestic cats. J. Am. Vet. Med. Assoc. 225, 1394–1398.

Otsu, N., 1979. A threshold selection method from gray-level histograms. IEEE Trans. Syst. Man Cybern. 9, 62–66.

Petry, G., Kruedewagen, E., Bach, T., Gasda, N., Krieger, K.J., 2011. Efficacy of Procox® oral suspension for dogs (0.1% emodepside and 2% toltrazuril) against experimental nematode (*Toxocara cati* and *Ancylostoma tubaeforme*) infections in cats. Parasitol. Res. 109 (Suppl. 1), S37L S43.

Reid, L.E., Dillon, A.R., Hathcock, J.T., Brown, L.A., Tillson, M., Wooldridge, A.A., 2012. High-resolution computed tomography bronchial lumen to pulmonary artery diameter ratio in anesthetized ventilated cats with normal lungs. Vet. Radiol. Ultrasound 53, 34–37.

Reinemeyer, C.R., Charles, S.D., Buch, J., Settje, T., Altreuther, G., Cruthers, L., McCall, J.W., Young, D.R., Epe, C., 2005. Evaluation of the efficacy of emodepside plus praziquantel topical solution against ascarid infections (*Toxocara cati* or *Toxascaris leonina*) in cats. Parasitol. Res. 97 (Suppl. 1), S41L S50.

Schenker, R., Bowman, D., Epe, C., Cody, R., Seewald, W., Strehlau, G., Junquera, P., 2007. Efficacy of a milbemycin oxime-praziquantel combination product against adult and immature stages of *Toxocara cati* in cats and kittens after induced infection. Vet. Parasitol. 145, 90–93.

Schnieder, T., Laabs, E.M., Welz, C., 2011. Larval development of *Toxocara canis* in dogs. Vet. Parasitol. 175, 193–206.

Sommerfelt, I.E., Cardillo, N., López, C., Ribicich, M., Gallo, C., Franco, A., 2006. Prevalence of *Toxocara cati* and other parasites in cats' faeces collected from the open spaces of public institutions: Buenos Aires, Argentina. Vet. Parasitol. 140, 296–301.

Spain, C.V., Scarlett, J.M., Wade, S.E., McDonough, P., 2001. Prevalence of enteric zoonotic agents in cats less than 1 year old in central New York State. J. Vet. Intern. Med. 15, 33–38.

Sprent, J.F., 1956. The life history and development of *Toxocara cati* (Schrank 1788) in the domestic cat. Parasitology 46, 54–78.

Swerczek, T.W., Nielsen, S.W., Helmboldt, C.F., 1970. Ascariasis causing pulmonary arterial hyperplasia in cats. Res. Vet. Sci. 11, 103–104.

Upchurch, D.A., Dillon, A.R., Brawner, W.R., Tillson, M., Johnson, C., 2010. Comparison of findings from radiography, histology, and serology for the diagnosis of pulmonary lesions: A retrospective study of 120 random source cats. In: Proceedings: Am. Heartworm Soc. Meet.

Wolken, S., Schaper, R., Mencke, N., Kraemer, F., Schnieder, T., 2009. Treatment and prevention of vertical transmission of *Toxocara cati* in cats with an emodepside/praziquantel spot-on formulation. Parasitol. Res. 105 (Suppl. 1), S75–S81.

Wooldridge, A.A., Dillon, A.R., Tillson, D.M., Zhong, Q., Barney, S.R., 2012. Isometric responses of isolated intrapulmonary bronchioles from cats with and without adult heartworm infection. Am. J. Vet. Res. 73, 439–446.

Yildiz, K., Başalan, M., Duru, O., Gökpinar, S., 2011. Antiparasitic efficiency of *Artemisia absinthium* on *Toxocara cati* in naturally infected cats. Turk. Parazitol. Derg. 35, 10–14.